Sedimentation of metals in Sundarban mangrove ecosystem: Dominant drivers and environmental risks

Jayjit Majumdar[1]*, Jayanta Kumar Biswas[1,2]*, Subhas Chandra Santra[3], AL. Ramanathan[4] and Filip M. G. Tack[5]

[1]Department of Ecological Studies, University of Kalyani, Kalyani, Nadia, West Bengal - 741235, India

[2]International Centre for Ecological Engineering, University of Kalyani, Kalyani, Nadia, West Bengal - 741235, India

[3]Department of Environmental Science, University of Kalyani, Kalyani, Nadia, West Bengal - 741235, India

[4]School of Environmental Sciences, Jawaharlal Nehru University, New Delhi- 110067, India

[5]Department of Green Chemistry and Technology, Ghent University, Ghent, Belgium

*Corresponding authors (J. Majumdar, e-mail: jayjitmajumdar@gmail.com; J.K. Biswas, e-mail: biswajoy2008@gmail.com)

Abstract

Metal contamination from upstream river water is a threat to coastal and estuarine ecosystem. The present study was undertaken to unveil sedimentation processes and patterns of heavy metal deposition along the salinity gradient of a tropical estuary and its mangrove ecosystem. Sediment columns from three representative sites of differential salinity, anthropogenic interference, and sediment deposition pattern were sampled and analyzed for grain size distribution and metal concentrations as a function of depth. Sediments were dominantly of silty-medium sand texture. A suite of fluvial and alluvial processes, and marine depositional forcing control the sediment deposition and associated heavy metal loading in this estuary. The depth profile revealed a gradual increase in heavy metal accumulation in recent top layer sediments and smaller fractions (silt + clay), irrespective of tidal regimes. Alluvial processes and long tidal retention favor accumulation of heavy metal(s). Enrichment factor (0.52-15), geo-accumulation index (1.4-5.8), and average pollution load index (PLI = 2.0) indicated moderate to higher heavy metal contamination status of this estuary. This study showed that alluvial processes acted as dominant drivers for the accumulation of metals in sediments, which prevailed over the influence of marine processes. Longer tidal retention of the water column favored

more accumulation of heavy metals. Metal accumulation in the sediments entails a potential risk of bioaccumulation and bio-magnification through the food web, and may increasingly impact estuarine ecology, economy, and ultimately human health.

Keywords: Estuary; metal contamination; sediment deposition; geo-accumulation; pollution load; environmental health

1. Introduction

Estuaries, as biologically highly productive areas, are very sensitive to natural and anthropogenic impacts. Deposition of upstream trace metal contamination mediated by alluvial processes is a threat to coastal and estuarine ecosystem (Sarkar et al., 2018). Metals enter into the estuarine sedimentary environment through both natural processes (erosion of ore-bearing rocks, windblown dust, volcanic activity, atmospheric deposition, forest fires, and subsequent alluvial transport) and anthropogenic activities (industrial discharge, application of agrochemicals, and subsequent runoff into rivers) (Abrahim and Parker, 2002; Islam et al., 2015a; Kibria et. al., 2016; Sarkar et al., 2017; Mitra et al., 2018). Sediment generally acts as a sink for metals. However, physical disturbances caused by natural factors such as coastal storm surges, bioturbation by sediment dwelling organisms, and physicochemical processes including diagenesis, changes in redox conditions and pH can turn sediment into a source of metals (Chatterjee et al., 2009; Brady et. al., 2014; Boehler et. al., 2017). Grain size of the sediments plays a paramount role in influencing metal diagenesis in sediments. Grain size and metal concentrations over depth reflect depositional patterns of sediment and associated metals over a large period (Chatterjee et al., 2007; Metge et al., 2010; Okoro et al., 2013; De Mahiques et al., 2013; Strady et. al., 2017). Hydrological processes in deltas and estuaries change continuously due to the seasonal and temporal variability of upstream water flow (Eissen et al., 2009; Schaider et al.; 2014). Temporally facial boundaries migrate, and transgression and regression processes appear to play pivotal roles in sedimentation (Reineck and Singh, 2012; Clarke et. al., 2014). The intensity of tidal influence, pace of sediment supply, power of hydrodynamic processes, local micro-tectonics, and sea level changes control processes of transgression-regression and configuration of basin sedimentation in the estuary (Reineck and Singh, 2012; Clarke et. al., 2014; Woodroffe et. al., 2016).

The Ganges delta is the largest delta in the world (Sarkar et al., 2017). It recharges the Sundarbans freshwater swamp forests ecoregion, the largest mangrove ecosystem in the world (Stanley and Hait, 2000; Banerjee et al., 2012). The Sundarbans has been recognized as an international area of outstanding universal value (World Heritage Site) by the United Nations Educational, Scientific and Cultural Organization

(UNESCO) and is recognized as an internationally important wetland site (Ramsar site) under the Ramsar Convention (Mitra et al. 2012; Rahman, 2012). Protected areas include Sundarbans National Park and Sajnakhali Wildlife Sanctuary in West Bengal, and Sundarbans East, Sundarbans South and Sundarbans West Wildlife Sanctuaries in Bangladesh, covering 15% of the total area (WWF, 2022). The Indian part is situated in the north-eastern part of the Bay of Bengal, and covering a surface area of 4,110 km² of which river, canals, and creeks occupy about 1,700 km² (Spalding et al., 1997; Alam et al., 2010). The Sundarban mangrove ecosystem stands as one of the most productive ecosystems in the world (Banerjee et al., 2012). It stabilizes sedimentary deposition from the upstream environment and acts as a buffer between seashore, lagoon, and estuary (Furukawa and Wolanski, 1996). Mass accumulation of sediment ranges from 0.41gcm^{-2} year^{-1} in the estuarine region to 0.66 gcm^{-2} year^{-1} in the mangrove regions (Ramanathan et al., 2009; Banerjee et al., 2012).

As a geochemically young and active tectonic river basin, Sundarban is recognized as a very sensitive and threatened ecosystem. This deltaic region is highly vulnerable to climate change-associated alterations in temperature, precipitation, salinity, and erosion (Sarkar et al., 2017). Metals from human activities enter the river Ganga and its tributaries as it flows through extensive regions impacted by agricultural activity, urbanization, and industry.

Sediment cores reflect historical contamination. Several studies investigated heavy metals in sediment and biota in Sundarban estuarine ecosystem during last few decades showing wide variations in their findings (Guhatahkurta and Kaviraj, 2000; Mukerjee et al., 2009; Rajkumar et al., 2012; Chakraborty et al., 2014; Kumar et al., 2016; Kader and Sinha, 2018; Mitra et al., 2018; Ranjan et al., 2018). But work on sedimentation process history and its relationship with metal accumulation is very limited (Jonathan et al., 2010; Silva Filho et al., 2011; Banerjee et al., 2012; Rajkumar et al., 2014; Kumar and Ramanathan, 2015).

To bridge the existing research gap the present study aimed to elucidate the pattern of sediment deposition along the salinity gradient of the central part of Indian Sundarban estuary, along with associated metal accumulation through sedimentgranulometric and heavy metals analyses, and appropriate validation for process factors analyses. The trace metal deposition in sediments was monitored to portray metal accumulation patterns, and provide a baseline for pollution surveillance in the metal-stressed fragile estuarine ecosystem.

2. Materials and methods

2.1. Sampling sites

Three sampling sites in the Sundarban estuary were selected based on the geographical location, tidal regime, and salinity gradient (Fig 1) to represent different sediment deposition scenarios. Shushunia island (site:

S1, 88.921° E/22.326°N) is in the northeastern part and receives mainly freshwater from the upstream region, whereas Moipith (Site: S2: 88.776° E/22.112° N) and Belmati islands (Site: S3, 88.748° E/22.066°N) are in the central to the southern part of the estuary subjected to longer tidal inundation (Chaterjee et al., 2013). Moipith island has a longer retention time of suspended sediment and is subjected to maximum anthropogenic disturbances (Alongi et al. 2005; Chaterjee et al., 2013; Singh et al., 2016). Shushunia and Belmati are covered with pristine mangrove vegetation (Ramanathan et al., 2009; Banerjee et al., 2012).

2.2. Sample collection, separation, and preservation

This study included (1) a broader sampling to assess metal distribution. For measuring metal enrichment in sediment in this estuary, surface sediment sampling was done from 42 different sampling locations and subsequently analysed for background value calculation of individual metals. 2) On three selected locations, undisturbed core samples were taken for a detailed study on metal deposition patterns. Three sampling sites differing in salinity, anthropogenic interference, and sediment deposition pattern were selected according to their strategic position in this estuary.

Sediment cores were collected from the tidal flat regions of the three study sites (S1, S2, and S3) during the low tide period. PVC (Polyvinyl chloride) pipes (150 cm length, 6.5 cm diameter) were manually inserted into the sediment up to a depth of 1 m with help of a woodenmallet. The top end of each pipe was covered with airtight screw caps and then gently extracted by hand with the help of a choking chain, without disturbing the sediment column trapped inside. The cores were then sliced by using a band saw. The sediment samples of different depths were removed using a measuring tape and clean spatula from pipes, sealed, transported to the lab, and kept under frozen conditions (-4ºC) until further analysis.

2.3. Sediment Granulometry

Separated sediment samples were air-dried and homogenized by gentle pounding with the help of a wooden mallet. They were sieved with ASTM sieve sets (250 µm, 125 µm, 63 µm, and pan) for 40 minutes at 25 ºC. Dry sieving of sediment samples was carried out using an electromagnetic vibratory sieve shaker Fritsch Analysette-3 Pro (Germany), to separate the fractions>250 µm (coarse sands),>125 µm (fine sands), 63-125 (very fine sands) and < 63 µm (silt + clay). Further separation of the fraction <63 µm was carried out using the Attenburg sedimentation cylinder method based on Stokes' law (Friedman, 1961). The granulometric data (Supplementary Table 1) were further processed using GRADISTAT version 4.0 (Blott and Pye, 2001) to compute textural parameter statistics such as mean (ϕ), standard deviation (σ1), skewness (Sk_1), and Kurtosis (K_G), to reconstruct the depositional environment at different depths (Supplementary Table 2). Linear discriminant function (LDF) and process factors such as Y1 (aeolian: beach), Y2 (beach: shallow marine), Y3 (shallow marine: fluvial), and Y4 (fluvial: turbidity current) were calculated (Table 1) for identification of the energy processes involved during deposition.

Process factors were interpreted using the following equations (Sahu, 1964; Angusamy and Rajamanickam, 2007):

$$\text{Y1 (aeolian: beach)} = -3.5688Mz + 3.7016\,\delta 1^2 - 2.0766\,Sk_1 + 3.1135\,K_G \quad (1)$$

$$\text{Y2 (beach: shallow marine)} = 16.6534Mz + 65.7091\,\delta 1^2 + 18.1071\,Sk_1 + 18.5043K_G \quad (2)$$

$$\text{Y3 (shallow marine: fluvial)} = 0.2852Mz - 8.7604\,\delta 1^2 - 4.8932\,Sk_1 + 0.0482K_G \quad (3)$$

$$\text{Y4 (fluvial: turbidity current)} = 0.7215\,Mz - 0.4030\delta 1^2 + 6.7322\,Sk_1 + 5.2927K_G \quad (4)$$

Where Mz stands for mean grain-size, $\delta 1$ stands for inclusive graphic standard deviation (sorting), Sk_1 stands for skewness, K_G stands for Kurtusis of size class.

Y1 would distinguish between aeolian deposition (Y1 < -2.7411) versus beach environment (Y1 > -2.7411), whereas Y2 distinguishes between beach deposition (Y2 < 65.365) and shallow agitated water deposition (Y2 < 65.365). Y3 reflects either a fluvial (deltaic) deposit (Y3 < -7.4190), or a shallow marine deposit (Y3 > -7.4190), and Y4 allows to differentiate between turbidity current (Y4 < 9.8433) and fluvial (deltaic) deposition (Y4 > 9.8433).

2.4. Determination of metal concentrations

The fine fraction of sediment (<63 µm) was subject to analysis of pseudo-total metal (Ca, Mg, Cu, Cr, Ni, Zn, and Mn) concentrations. Sediment samples were air-dried. Before sample digestion, glassware was washed with 2% HNO_3 (v/v), rinsed with de-ionized water, and oven-dried. About 0.5 g of sediment sample was taken into clean, dry digestion tubes and 5 ml of concentrated HNO_3 (15.8 M Merck, Germany) was added. The mixture was allowed to stand overnight under a fume hood. On the following day, the digestion tubes were placed on a heating block and heated at 60°C for 2 hr. The tubes were then allowed to cool at room temperature. About 3 ml of concentrated (36.5 N) H_2SO_4 (Merck, Germany) and 2 ml of concentrated perchloric acid ($HClO_4$) (69%, Merck, Germany) were added to digestion mixtures. The tubes were heated at 160°C for about 4–5 hours till the dense white fume of $HClO_4$ was emitted. The contents were then cooled down, diluted to 25 ml with de-ionized water, filtered (Whatman No. 42), and stored in polyethylene bottles (Bhattacharya et al., 2010; Bhattacharya et al., 2013; Lin et al., 2013).

2.5. Analytical quality control

Sediment samples were digested and analyzed in triplicate to check procedural and analytical accuracy. Besides sediment samples, sample blanks and Standard Reference Materials (SRM) were analyzed following the same procedures as stated above for the samples. SRM's included BCR- CRM 277r (estuarine sediment for Fe, Cr, Fe, Mn, Ni, and Zn) and BCR 129 (Hay powder for Ca and Mg), both obtained from the Institute for Reference Materials and Measurements (Belgium, European Union). Up to 97.13- 98.37% recovery was obtained for the certified metals in SRM BCR- CRM 277r, whereas for SRM BCR- 129, recoveries of 96.28% for Mg and 98.31% for Ca were obtained.

2.6. Quantitative estimation of metal pollution and possible threat identification

The Pollution load index (PLI) was calculated for characterizing the status of metal pollution in this estuary concerning the background concentration and contamination factor (CF) of that particular metal (Islam et al., 2015a; Islam et al., 2015b; Antoniadis et al., 2016). This was calculated according to the method developed by Tomlinson et al (1980), as:

$$CF = C\ metal / C\ background\ value \quad (5)$$

$$PLI = n \sqrt{(CF1 x CF2 x CF3 x \ldots x CFn)} \quad (6)$$

Where, CF = contamination factor, n = number of metals, C metal = metal concentration in polluted sediments, C Background value = background value of that metal (mean calculated from surface sediment from 42 locations and checked with existing literature). A PLI value of > 1 is interpreted as "generally polluted with metals", whereas <1 indicates "no pollution".

For the identification of accumulation trends of heavy metals in sediments for prolonged periods, the geo- accumulation indices (*Igeo*) were calculated according to Muller (1979).

$$Igeo = \ln (Cn / 1.5\ Bn) \quad (7)$$

Where, Cn = Measured concentration of metal in the sediment, Bn = Geochemical background value in the average of element n. The mean concentration of concerned metal was calculated based on 42 different composite samples collected from Sundarban mangrove, which was subsequently used as Bn value. Factor 1.5 is used as a moderating factor accounting for the possible variations of the background data due to lithological variations.

Iron is an important metal in any type of sediment/ soil system as it plays a vital role in agglomeration and accumulation of other heavy metals (Schaider et al., 2014; Huerta-Diaz et al., 2014). Therefore, enrichment factor/s (EF) of metals were calculated based on the reference element (Fe). The method of calculation of EF is expressed as follows (Feng et al., 2004; Barbieri, 2016).

$$EF = (Metal/RE)\ soil / (Metal/RE)\ background \quad (8)$$

Where RE is the concentration of Reference Element (Fe).

On the basis of calculating *Igeo**and EF# values the contamination status of the sediments was assessed following the classification scale represented below:

* I_{geo}>5, extremely contaminated; 4–5, strongly to extremely strongly contaminated; 3–4, strongly contaminated; 2–3, moderately to strongly contaminated; 1–2, moderately contaminated; 0–1, uncontaminated to moderately contaminated; <0, uncontaminated (Muller, 1979; Essien et. al., 2009; Barbieri, 2016)

EF < 1, no enrichment; EF < 3, minor enrichment; EF = 3–5, moderate enrichment; EF = 5–10, moderately severe enrichment; EF = 10–25, severe enrichment; EF = 25–50, very severe enrichment and EF > 50 extremely severe enrichments (Birth, 2003; Barbieri, 2016).

3. Results and discussion

3.1. Sedimentation process

Irrespective of depth, sediments at all sites are generally classified as "coarse-silty-medium sand" (Shepard, 1954) (Texture analysis provided in SI, Supplementary Table 1 and Supplementary Fig. 1). This agrees with previous work in this estuary (Mukherjee et al., 2009; Rajkumar et al., 2012). Most samples are moderately sorted, fine to very coarse skewed, and very platykurtic (Supplementary Table 2).

Linear discriminant function (LDF) analysis revealed that irrespective of sampling location and depth (Table 1), average Y1 (aeolian: beach) values at site S1, S2, and S3 were calculated as -5.047, -5.335, and +5.154 respectively; Y1 values less than -2.7411 imply that the aeolian process is in operation (Table 1). Irrespective of sample depth in three sampling locations Y2 (beach: shallow marine) values also have crossed the threshold 65.3650, indicating an agitated regime of the shallow marine environment. Onsite S1, calculated Y3 (Shallow marine: fluvial process) ranged between -9.720 (66-72 cm depth) to -5.350 (12-18 cm depth) indicating shallow marine deposition prevailing at this site. At the depth of 0-6, 6-12, 24-30 cm, and 66-72 cm Y3 is less than -7.4190, which points towards fluvial deposition while the remaining samples are indicative of shallow marine deposition. This suggests that recent sediments at site S1 are predominantly subjected to fluvial influence. In the case of site S2, an Y3 value lower than -7.4190 irrespective of depth suggests only fluvial deposition in this part of the estuary. For site S3, samples collected from 0-24 cm and 72-78 cm depth are derived from shallow marine deposit while the rest bears the testimony of fluvial deposit. Samples from S1 and S3 have Y4 (fluvial: turbidity current) values less than 9.8433, which implies that these two sites have turbidity current-driven deposition. The central part of the estuary (S2) experiences more deltaic (fluvial) influence than marine influence.

Previous studies revealed that tidal retention time is high in this estuary particularly central part of this estuary (Singh et al., 2016; Chatterjee et al., 2020). Overall estuarine sediments are subjected to fluvial processes with alternate tidal and marine influence. The results indicated a gradual decrease in freshwater input due to the lower flow rate of the river and its tributaries in the northern part of this estuary. This has been attributed to the diversion of the water stream for diverse human usages leading to prolonged tidal and marine influence (Mitra et al., 2009; Smith et al., 2009). The gradual erosion of comparatively low salinity-loving mangrove plant species (such as *Heritiera* sp.) and changing species diversity also support the hypothesis of less freshwater supply to this estuary (Zaman et al., 2013; Awal, 2014).

3.2. Metal concentration

Depth profile analysis of alkaline earth metals (calcium and magnesium) gives a clear picture of depositional cycles of these metals in this estuary (Fig. 3). In the case of sites S1 and S2, calcium deposition remains almost similar whereas site S3 reveals increasing Ca deposition over time. From the alkaline earth metals content, it becomes evident that there is a marine influence active in S3 and to some extent in S2. Periodic alteration (increase and decrease) in both Ca, and Mg concentrations is apparent at site S1. Thus both the marine and fluvial forces and processes are acting as drivers of change in metal concentrations in this region.

Recent sediments in Shushunia island (S1) revealed a lower Fe concentration in comparison to older sediments (Fig.2), whereas concentrations of Cr, Mn, Zn and Cu were higher in recent sediments. The concentrations of these metals appeared to build up with the freshwater from the upstream region carrying loads of metals. Therefore, the concentrations of heavy metals increased in sediment deposited downstream. The concentration of Ni at the S1 site initially decreased from top to bottom, and then increased again. In contrast, Ni concentration in recent sediments at site S2 and S3 showed a clear decreasing trend. In the sediment core from the Moipith island (S2) copper and zinc presented a rather random depositional pattern with an indication of increased deposition in recent sediments. Although the profile of Fe also revealed important variability, there was an overall a decreasing trend in the more recently deposited sediments. For Mn (452 - 641 mg kg^{-1}) and Cr (51 - 75 mg kg^{-1}), there was a steady but slow increasing trend in the depth profile at Moipith island (S2). Core sediment collected from the Belmati island (S3) had a steadily increasing trend in Ca and Mg concentration in recent sediment profile along with concentrations of Cu (127-209 mg kg^{-1}), Zn (186.5-261.5 mg kg^{-1}), and Mn (492-1059 mg kg^{-1}). Such a consistent increase in Ca and Mg concentration reflects increasing marine influence at this particular sampling site. Most of the metals reveal an overall increasing trend of deposition in recent sediments, which is a clear indication of a gradual buildup of those metals attributed to the upstream input (Essien et al, 2009; Schaider et al., 2014; Huerta Diaz et al., 2014). Because Fe/Mn oxides are an important binding phase for metals, increased heavy metal concentrations can be expected with increased Fe concentrations (Turner, 2000; Essien et al., 2009; Xie et. al, 2016). However, in the present study, Fe concentration is decreasing in recent sediments in all the three selected locations, which seems to be contradictory to the findings of previous works (Islam et al., 2004; Mitra et al., 2009; Jonathan et al., 2010; Banerjee et al., 2012; Awal et al., 2014) on metal deposition/ accumulation in the sediment. Studies conducted by Jonathan et al. (2010) and Banerjee et al. (2012) reported over 4.5- 5.5 % of Fe in central part of the estuary in recent sediments. Whereas in case of the present study recent sediments have 3- 4.2 % of Fe. This reduction of Fe concentration may be due to several factors such as thermodynamic scavenging of other metals along with Mn, flocculation with humic substances and subsequent disintegration of humic/fulvic acid - metal complexes and resolubilization (L'her Roux et al., 1998; Kumar and Ramanthan, 2015; Oldham et al., 2019).

3.3. Metal pollution threat

The average Pollution load index (PLI) of the metals mixed feature according to the depth (Fig. 4) in three sampling locations. The PLI value in S1 ranges from 1.81 to 2.90 with an average of 2.10. In case of S2 and S3 PLI ranges from 1.64 to 2.3 (average 1.80) and from 1.89 to 2.49 (average 2.13) respectively. The PLI values indicate high pollution load in this study area and the Belamati region (S3) is the most polluted one. However, recent sediments of all three sampling sites have higher PLI values compared to older sediments implying transition of pollution load from moderate to high pollution in near future. The *Igeo* values at all three designated locations indicate that the current level of accumulation of tested metals like Cr, Mn, and Ni is very high in this estuary. The *Igeo* values of different metals in recent sediments are higher in comparison to older sediment. At Shushunia island the mean *Igeo* values for Cr, Mn, Zn, Cu, and Ni are 3.44, 2.45, 3.57, 2.22, and 5.13 respectively considering all sediment depths, whereas, in the case of Moipith and Belmati, they are 3.29, 1.14, 3.57, 2.26, 5.55 and 3.45, 1.86, 3.60, 5.74 respectively (Fig. 5) suggesting moderate to strongly polluted condition (Muller, 1979; Barbieri, 2016). A similar outcome is obtained by calculating metal enrichment factors (EF) for the three core sediments (Fig. 6). From the EF analysis it was found that this estuary is highly polluted by Ni (4.56- 14.77) followed by moderate to minor enrichment by Chromium (1.28- 4.9), Zn (1.62- 4.57), Cu (0.54-2.92), and Mn (0.40 - 1.63). Recent sediment had higher PLI, *Igeo*, and EF values suggesting a higher rate of deposition of metals during recent years. Increase of metals concentration in recent sediments is due to effluent released from power plant operation, harbor activities, metallurgy industries, local small scale electroplating industries and constant movements of fishing and touring boats in this estuary ((Banerjee et al., 2012; Mitra et al., 2009). From these observations, it can be concluded that there is a periodic pattern of metal deposition in this estuary in the case of all three sampling locations, and a similar trend can be observed in estuaries around the world (Birch and Olmos, 2008; Alyazichi et al., 2017). For example, the trace metal profiles of surface sediments of the estuaries of Georges River, Southern Sydney, and New South Wales, Australia corroborate present findings, created by the discharge from the catchment area, bay morphology, and sediment types (sand, silt, and clay) (Birch and Olmos, 2008; Alyazichi et al., 2017). Comparison of sediment metal content of different estuaries and mangroves around the world (Table 2) gives a comparative picture of heavy metals load in sediment of Sundarban mangrove estuary. The EF values are simultaneously increasing in Shushunia (S1) and Belmati island (S3) and have a more or less uniform cyclic pattern of deposition. The study establishes Shushunia island (S1) as the most polluted one with the highest heavy metal load in the sediments. Due to its unique geographical location (upstream) for being more exposed to water from different tributaries and distributaries of the Matla River and comparatively longer retention time (Alongi, 2005; Singh et al., 2016; Chatterjee et al., 2020) S1 experienced higher accumulation of heavy metal in silt clay fraction while rest remaining in water column later could settle in the sediments. The upstream region of this estuary is densely populated and diverse industries are present. Wastewater from those industries and agricultural runoff add the bulk of heavy metals in this estuary (Guhathakurta and Kaviraj, 2000; Turner, 2000; Saha et al., 2001; DeMahiques et al., 2013). Reports suggested bioaccumulation and biomagnification of metals in plants, bottom-dwelling fauna, commercially important fish, and shellfish, indicating a threat to this ecosystem (Ramanathan et al., 2009; Alam et al., 2010; Silva Filho et al., 2011; Barua et al., 2011; Chaudhuri et al., 2014; Kader and Sinha, 2018). Control of trace metals released from upstream, and integrated ecotoxicological assessment are warranted for identifying and averting pollution in this stressed and sensitive estuarine environment.

4. Conclusions

The Sundarbans freshwater swamp forests ecoregion is subjected to input of trace metals from the upstream region, which subsequently get deposited in estuarine and mangroves areas. Metals including Cu, Cr, Zn and Mn have an overall increasing trend of accumulation in more recent sediment. The central part of the estuary, which adjoins the Malta River, receives more sediment and heavy metals load contributed by the upstream region. This region also has a higher sedimentation rate due to longer retention of water column influenced by the turbidity process. Longer retention of suspended particles in water under the influence of the turbidity current ensures a higher accumulation of heavy metals in the estuarine sediment attributed mainly to smaller sediment particles fromthe upstream region. This study shows that alluvial processes act as dominant drivers for the accumulation of metals in the studied areas of the Sundarbans ecoregion sediments. Although changes in sediment deposition patterns reflect an increasing marine influence in this estuary. Stable isotope and tracer isotope analysis of metals would be very useful for a better understanding of the temporal deposition and geo-accumulation of trace metals in this estuary. Since metals are known for their high potential of bioaccumulation and biomagnification and Sundarban provides the home for large numbers of edible fish and shellfish population, it can pose a potential risk to public health.

Acknowledgment

The authors are grateful to the University Grant Commission (India) for providing funding for experiments and fellowship and the Department of Environmental Science, University of Kalyani for providing necessary laboratory facilities. Authors are very much thankful to anonymous reviewers for their valuable comments and suggestions for improving this manuscript from its previous versions.

Availability of data and material

All used data are presented in tables and figures in the paper.

Declaration

Conflicts of interest

The authors have no conflicts of interest to declare that are relevant to the content of this article.

References

Abrahim, G., & Parker, R. (2002). Heavy-metal contaminants in Tamaki Estuary: impact of city development and growth, Auckland, New Zealand. *Environmental Geology*, *42*(8), 883-890. https://doi.org/10.1007/s00254-002-0593-0

Adebowale, K. O., Agunbiade, F. O., & Olu-Owolabi, B. I. (2009). Trace metal concentrations, site variations and partitioning pattern in water and bottom sediments from coastal area: a case study of Ondo coast, Nigeria. *Environmental Research Journal*, *3*(2), 46-59.

Alam, M. A., Gomes, A., Sarkar, S. K., Shuvaeva, O. V., Vishnevetskaya, N. S., Gustaytis, M. A., Bhattachariya, B. D. & Godhantaraman, N. (2010). Trace metal bioaccumulation by soft-bottom polychaetes (Annelida) of Sundarban Mangrove Wetland, India and their potential use as contamination indicator. *Bulletin of environmental Contamination and Toxicology*, *85*(5), 492-496.https://doi.org/10.1007/s00128-010-0110-1

Alongi, D. M., Ramanathan, A. L., Kannan, L., Tirendi, F., Trott, L. A., & Prasad, M. B. K. (2005). Influence of human-induced disturbance on benthic microbial metabolism in the Pichavaram mangroves, Vellar–Coleroon estuarine complex, India. *Marine biology*, *147*(4), 1033-1044.https://doi.org/10.1007/s00227-005-1634-5

Angusamy, N. & Rajamanickam, G.V. (2007). Coastal processes of Central Tamil Nadu, India: clues from grain size studies. *Oceanologia* 49(1), 41-57.

Antoniadis, V., Golia, E. E., Shaheen, S. M., & Rinklebe, J. (2017). Bioavailability and health risk assessment of potentially toxic elements in Thriasio Plain, near Athens, Greece. *Environmental geochemistry and health*, *39*(2), 319-330. https://doi.org/10.1007/s10653-016-9882-5

Awal, M. A. (2014). Invention on correlation between the chemical composition of the surface sediment and water in the mangrove forest of the Sundarbans, Bangladesh, and the regeneration, growth and dieback of the forest trees and people health. *Science Innovation 2*(2), 11-21. https://doi.org/10.11648/j.si.20140202.11

Banerjee, K., Senthilkumar, B., Purvaja, R., & Ramesh, R. (2012). Sedimentation and trace metal distribution in selected locations of Sundarbans mangroves and Hooghly estuary, Northeast coast of India. *Environmental geochemistry and health*, *34*(1), 27-42. https://doi.org/10.1007/s10653-011-9388-0

Barbieri, M., (2016). The importance of enrichment factor (EF) and geoaccumulation index (Igeo) to evaluate the soil contamination. *Journal of Geology and Geophysics5*(1), 237. http://dx.doi.org/10.4172/2381-8719.1000237

Barua, P., Mitra, A., Banerjee, K. & Chowdhury, M. S. N. (2011). Seasonal variation of heavy metals accumulation in water and oyster (*Saccostrea cucullata*) inhabiting central and western sector of Indian sundarbans. *Environmental Research Journal*, *5*(3), 121-130. http://dx.doi.org/10.3923/erj.2011.121.130

Bhattacharya, P., Samal, A. C., Majumdar, J., & Santra, S. C. (2010). Accumulation of arsenic and its distribution in rice plant (Oryza sativa L.) in Gangetic West Bengal, India. *Paddy and Water Environment*, *8*(1), 63-70. https://doi.org/10.1007/s10333-009-0180-z

Bhattacharya, P., Samal, A. C., Majumdar, J., Banerjee, S., & Santra, S. C. (2013). In vitro assessment on the impact of soil arsenic in the eight rice varieties of West Bengal, India. *Journal of hazardous materials*, *262*, 1091-1097. https://doi.org/10.1016/j.jhazmat.2012.09.004

Birch, G. F., & Olmos, M. A. (2008). Sediment-bound heavy metals as indicators of human influence and biological risk in coastal water bodies. *ICES journal of marine science*, *65*(8), 1407-1413. https://doi.org/10.1093/icesjms/fsn139

Birth, G. (2003). A scheme for assessing human impacts on coastal aquatic environments using sediments. In Woodcoffe, C. D., & FurnessR. A. (Eds.) *Coastal GIS*, Wollongong University Papers in Center for Maritime Policy, 14, Wollongong, Australia.

Blott, S. J., & Pye, K. (2001). GRADISTAT: a grain size distribution and statistics package for the analysis of unconsolidated sediments. *Earth surface processes and Landforms*, *26*(11), 1237-1248. https://doi.org/10.1002/esp.261

Boehler, S., Strecker, R., Heinrich, P., Prochazka, E., Northcott, G. L., Ataria, J. M., Leusch, F. D. L, Braunbeck, T. & Tremblay, L. A. (2017). Assessment of urban stream sediment pollutants entering estuaries using chemical analysis and multiple bioassays to characterise biological activities. *Science of the Total Environment*, *593*, 498-507. https://doi.org/10.1016/j.scitotenv.2017.03.209

Brady, J. P., Ayoko, G. A., Martens, W. N., & Goonetilleke, A. (2014). Enrichment, distribution and sources of heavy metals in the sediments of Deception Bay, Queensland, Australia. *Marine pollution bulletin*, *81*(1), 248-255. https://doi.org/10.1016/j.marpolbul.2014.01.031

Burton Jr, G. A., & Scott, K. J. (1992). Sediment toxicity evaluations. *Environmental science & technology*, *26*(11), 2068-2075. https://doi.org/10.1021/es00035a002

Chakraborty, P., Ramteke, D., Chakraborty, S., & Nagender Nath, B. (2014). Changes in metal contamination levels in estuarine sediments around India - An assessment. *Marine Pollution Bulletin*, *78*(1–2), 15–25. https://doi.org/10.1016/j.marpolbul.2013.09.044

Chatterjee, M., Massolo, S., Sarkar, S. K., Bhattacharya, A. K., Bhattacharya, B. D., Satpathy, K. K., & Saha, S. (2009). An assessment of trace element contamination in intertidal sediment cores of Sunderban mangrove wetland, India for evaluating sediment quality guidelines. *Environmental monitoring and assessment*, *150*, 307-322. https://doi.org/10.1007/s10661-008-0232-7

Chatterjee, M., Shankar, D., Sen, G. K., Sanyal, P., Sundar, D., Michael, G. S., Chatterjee, A., Amol, P., Mukherjee, D., Suprit, K., Mukherjee, A., Vijith, V., Chatterjee, S., Basu, A., Das, M., Chakraborti, S., Kalla, A., Misra, S. K., Mukhopadhyay, S., Mandal, G., & Sarkar, K. (2013). Tidal variations in the Sundarbans estuarine system, India. *Journal of Earth System Science*, *122*(4), 899-933. https://doi.org/10.1007/s12040-013-0314-y

Chatterjee, M., Silva Filho, E. V., Sarkar, S. K., Sella, S. M., Bhattacharya, A., Satpathy, K. K., Prasad, M. V. R., Chakraborty, S. & Bhattacharya, B. D. (2007). Distribution and possible source of trace elements in the sediment cores of a tropical macrotidal estuary and their ecotoxicological significance. *Environment international*, *33*(3), 346-356. https://doi.org/10.1016/j.envint.2006.11.013

Chaudhuri, P., Nath, B., & Birch, G. (2014). Accumulation of trace metals in grey mangrove Avicennia marina fine nutritive roots: the role of rhizosphere processes. *Marine pollution bulletin*, *79*(1-2), 284-292. https://doi.org/10.1016/j.marpolbul.2013.11.024

Clarke, D. W., Boyle, J. F., Lario, J., & Plater, A. J. (2014). Meso-scale barrier estuary disturbance, response and recovery behaviour: Evidence of system equilibrium and resilience from high-resolution particle size analysis. *The Holocene*, *24*(3), 357-369. https://doi.org/10.1177/0959683613518597

Curray, J. R. (1964). Transgressions and regressions. In R.L. Miller (Eds.), *Papers inMarine Geology*, (175-203). New York: Macmillan.

De Mahiques, M. M, Figueira, R. C. L, Salaroli, A. B, Alves, D. P. V. & Gonçalves, C. (2013). 150 years of anthropogenic metal input in a Biosphere Reserve: the case study of the Cananéia-Iguape coastal system, Southeastern Brazil. *Environmental Earth Sciences*, *68*(4). 1073-1087. https://doi.org/10.1007/s12665-012-1809-6

Dung, T. T. T., Linh, T. M., Chau, T. B., Hoang, T. M., Swennen, R., & Cappuyns, V. (2019). Contamination status and potential release of trace metals in a mangrove forest sediment in Ho Chi Minh City, Vietnam. *Environmental Science and Pollution Research*, *26*(10), 9536-9551. https://doi.org/10.1007/s11356-019-04355-3

Essien, J. P., Antai, S. P., & Olajire, A. A. (2009). Distribution, seasonal variations and ecotoxicological significance of heavy metals in sediments of cross river estuary mangrove swamp. *Water, Air, and Soil Pollution*, *197*(1), 91-105. https://doi.org/10.1007/s11270-008-9793-x

Feng, H., Han, X., Zhang, W., & Yu, L. (2004). A preliminary study of heavy metal contamination in Yangtze River intertidal zone due to urbanization. *Marine pollution bulletin*, *49*(11-12), 910-915. https://doi.org/10.1016/j.marpolbul.2004.06.014

Folk, R. L., & Ward, W. C. (1957). Brazos River bar [Texas]; a study in the significance of grain size parameters. *Journal of sedimentary research*, *27*(1), 3-26. https://doi.org/10.1306/74D70646-2B21-11D7-8648000102C1865D

Friedman, G. M. (1961). Distinction between dune, beach, and river sands from their textural characteristics. *Journal of Sedimentary Research*, *31*(4), 514-529. https://doi.org/10.1306/74D70BCD-2B21-11D7-8648000102C1865D

Friske, P. W. B., Rencz, A. N., Ford, K. L., Kettles, I. M., Garrett, R. G., Grunsky, E. C., McNeil, R.J. & Klassen, R. A. (2013). Overview of the Canadian component of the North American Soil Geochemical Landscapes Project with recommendations for acquiring soil geochemical data for environmental and human health risk assessments. *Geochemistry: Exploration, Environment, Analysis*, *13*(4), 267-283. https://doi.org/10.1144/geochem2012-140

Furukawa, K., & Wolanski, E. (1996). Sedimentation in mangrove forests. *Mangroves and salt marshes*, *1*(1), 3-10. https://doi.org/10.1023/A:1025973426404

Guhathakurta, H., & Kaviraj, A. (2000). Heavy metal concentration in water, sediment, shrimp (*Penaeus monodon*) and mullet (*Liza parsia*) in some brackish water ponds of Sunderban, India. *Marine Pollution Bulletin*, *40*(11), 914-920. https://doi.org/10.1016/S0025-326X(00)00028-X

Huang, P., Li, T. G., Li, A. C., Yu, X. K., & Hu, N. J. (2014). Distribution, enrichment and sources of heavy metals in surface sediments of the North Yellow Sea. *Continental shelf research*, *73*, 1-13. https://doi.org/10.1016/j.csr.2013.11.014

Huerta-Diaz, M. A., Muñoz-Barbosa, A., Otero, X. L., Valdivieso-Ojeda, J., & Amaro-Franco, E. C. (2014). High variability in geochemical partitioning of iron, manganese and harmful trace metals in sediments of the mining port of Santa Rosalia, Baja California Sur, Mexico. *Journal of Geochemical Exploration*, *145,* 51-63. https://doi.org/10.1016/j.gexplo.2014.05.014

Islam, M. L., Alam, M. J., Rheman, S., Ahmed, S. U., & Mazid, M. A. (2004). Water quality, nutrient dynamics and sediment profile in shrimp farms of the Sundarbans mangrove forest, Bangladesh. *Indian Journal of Marine Sciences*, *33*(2), 170-176. http://hdl.handle.net/123456789/1663

Islam, M. S., Ahmed, M. K., Raknuzzaman, M., Habibullah-Al-Mamun, M., & Islam, M. K. (2015[a]). Heavy metal pollution in surface water and sediment: a preliminary assessment of an urban river in a developing country. *Ecological indicators*, *48*, 282-291. https://doi.org/10.1016/j.ecolind.2014.08.016

Islam, S., Ahmed, K. M., Habibullah-Al-Mamun, M., & Masunaga, S. (2015[b]). Potential ecological risk of hazardous elements in different land-use urban soils of Bangladesh. *Science of the total environment*, *512*, 94-102. https://doi.org/10.1016/j.scitotenv.2014.12.100

Jonathan, M. P., Sarkar, S. K., Roy, P. D., Alam, M. A., Chatterjee, M., Bhattacharya, B. D., Bhattachairya, A., & Satpathy, K. K. (2010). Acid leachable trace metals in sediment cores from Sunderban Mangrove Wetland, India: an approach towards regular monitoring. *Ecotoxicology*, *19*(2), 405-418. https://doi.org/10.1007/s10646-009-0426-y

Kader, A., & Narayan Sinha, S. (2018). Heavy metal contamination in the sediment and plants of the Sundarbans, India. *Chemistry and Ecology*, *34*(6), 506–518. https://doi.org/10.1080/02757540.2018.1462344

Kalantzi, I., Papageorgiou, N., Sevastou, K., Black, K. D., Pergantis, S. A., & Karakassis, I. (2014). Metals in benthic macrofauna and biogeochemical factors affecting their trophic transfer to wild fish around fish farm cages. *Science of the total environment*, *470*, 742-753. https://doi.org/10.1016/j.scitotenv.2013.10.020

Kibria, G., Hossain, M. M., Mallick, D., Lau, T. C., & Wu, R. (2016). Trace/heavy metal pollution monitoring in estuary and coastal area of Bay of Bengal, Bangladesh and implicated impacts. *Marine pollution bulletin*, *105*(1), 393-402. https://doi.org/10.1016/j.marpolbul.2016.02.021

Kumar, A., & Ramanathan, A. L. (2015). Speciation of selected trace metals (Fe, Mn, Cu and Zn) with depth in the sediments of Sundarban mangroves: India and Bangladesh. *Journal of Soils and Sediments*, *15*(12), 2476–2486. https://doi.org/10.1007/s11368-015-1257-5

Kumar, A., Ramanathan, A. L., Prasad, M. B. K., Datta, D., Kumar, M., & Sappal, S. M. (2016). Distribution, enrichment, and potential toxicity of trace metals in the surface sediments of Sundarban mangrove ecosystem, Bangladesh: a baseline study before Sundarban oil spill of December, 2014. *Environmental Science and Pollution Research*, *23*(9), 8985–8999. https://doi.org/10.1007/s11356-016-6086-6

L’her Roux, L. L., Le Roux, S. L., & Appriou, P. (1998). Behaviour and speciation of metallic species Cu, Cd, Mn and Fe during estuarine mixing. *Marine Pollution Bulletin*, *36*(1), 56–64. https://doi.org/10.1016/S0025-326X(98)90033-9

Lin, Y. C., Chang-Chien, G. P., Chiang, P. C., Chen, W. H., & Lin, Y. C. (2013). Multivariate analysis of heavy metal contaminations in seawater and sediments from a heavily industrialized harbor in Southern Taiwan. *Marine pollution bulletin*, *76*(1-2), 266-275. https://doi.org/10.1016/j.marpolbul.2013.08.027

Liu, J., Wu, H., Feng, J., Li, Z., & Lin, G. (2014). Heavy metal contamination and ecological risk assessments in the sediments and zoobenthos of selected mangrove ecosystems, South China. *Catena*, *119*, 136-142. https://doi.org/10.1016/j.catena.2014.02.009

Metge, D. W., Harvey, R. W., Aiken, G. R., Anders, R., Lincoln, G., & Jasperse, J. (2010). Influence of organic carbon loading, sediment associated metal oxide content and sediment grain size distributions upon *Cryptosporidium parvum* removal during riverbank filtration operations, Sonoma County, CA. *water research*, *44*(4), 1126-1137. https://doi.org/10.1016/j.watres.2009.11.033

Mitra, A., Barua, P., Zaman, S., & Banerjee, K. (2012). Analysis of trace metals in commercially important crustaceans collected from UNESCO protected world heritage site of Indian Sundarbans. *Turkish journal of fisheries and aquatic sciences*, *12*(1), 53-66. https://dergipark.org.tr/en/pub/trjfas-ayrildi/issue/13270/160276

Mitra, A., Gangopadhyay, A., Dube, A., Schmidt, A. C., & Banerjee, K. (2009). Observed changes in water mass properties in the Indian Sundarbans (northwestern Bay of Bengal) during 1980–2007. *Current Science*, 1445-1452.

Mitra, S., Sarkar, S. K., Raja, P., Biswas, J. K., & Murugan, K. (2018). Dissolved trace elements in Hooghly (Ganges) River Estuary, India: Risk assessment and implications for management. *Marine pollution bulletin*, *133*, 402-414. https://doi.org/10.1016/j.marpolbul.2018.05.057

Mukherjee, D., Mukherjee, A., & Kumar, B. (2009). Chemical fractionation of metals in freshly deposited marine estuarine sediments of sundarban ecosystem, India. *Environmental geology*, *58*(8), 1757-1767. https://doi.org/10.1007/s00254-008-1675-4

Muller, G., (1979). Schwermetalle in den sediments des Rheins-Veranderungen seitt 1971. *Umschaun*. *79*(24), 778–783.

Nath, D., Mishra, R.N., Mandal, S., Saha, K. & Biswas, D.K. (2003). Heavy metal contents in Sundarban estuaries. *Journal of the Inland Fisheries Society of India35*(1), 78-84.

Ohimain, E. I., Olu, D. S., & Abah, S. O. (2009). Bioleaching of heavy metals from abandoned mangrove dredged spoils in the Niger delta; A Laboratory Study. *World Applied Sciences Journal*, *7*(9), 1105-1113.

Okoro, H. K., Fatoki, O. S., Adekola, F. A., Ximba, B. J., Snyman, R. G., & Mdokwana, B. W. (2013). The Effect of Particle Sizes on Metal Accumulation in the Marine Sediments of Cape Town Harbour. *Journal of North Carolina Academy of Science*, *129*(3), 115-125. https://doi.org/10.7572/2167-5880-129.3.115

Oldham, V. E., Siebecker, M. G., Jones, M. R., Mucci, A., Tebo, B. M., & Luther, G. W. (2019). The Speciation and Mobility of Mn and Fe in Estuarine Sediments. *Aquatic Geochemistry*, *25*(1–2), 3–26. https://doi.org/10.1007/s10498-019-09351-0

Rabee, A. M., Al-Fatlawy, Y. F., Abd, A. A. H. N., and Nameer, M. (2011). Using Pollution Load Index (PLI) and Geoaccumulation Index (I-Geo) for the Assessment of Heavy Metals Pollution in Tigris River Sediment in Baghdad Region. *Journal of Al-Nahrain University, 14*(4), 108-114. https://anjs.edu.iq/index.php/anjs/article/view/772

Rajkumar, K., Ramanathan, A. L., & Behera, P. N. (2012). Characterization of clay minerals in the Sundarban mangroves river sediments by SEM/EDS. *Journal of the Geological Society of India*, *80*(3), 429-434. https://doi.org/10.1007/s12594-012-0161-5

Rajkumar, K., Ramanathan, A. L., Behera, P. N., & Chidambaram, S. (2014). Preliminary studies on the characterization of clay minerals in the Sundarban mangrove core sediments, West Bengal, India. *Arabian Journal of Geosciences*, *7*(2), 537-544. https://doi.org/10.1007/s12517-012-0787-z

Raju, K. V., Somashekar, R. K., & Prakash, K. L. (2012). Heavy metal status of sediment in river Cauvery, Karnataka. *Environmental monitoring and assessment*, *184*(1), 361-373. https://doi.org/10.1007/s10661-011-1973-2

Ram, S. S., Aich, A., Sengupta, P., Chakraborty, A., & Sudarshan, M. (2018). Assessment of trace metal contamination of wetland sediments from eastern and western coastal region of India dominated with mangrove forest. *Chemosphere*, *211*, 1113-1122. https://doi.org/10.1016/j.chemosphere.2018.07.201

Ramanathan, A.L., Rajkumar, K., Majumdar, J., Singh, G., Behera, P.N., Santra, S.C., & Chidambaram, S. (2009). Textural characteristics of the surface sediments of a tropical mangrove Sundarban ecosystem India. *Indian Journal of Geomarine Sciences38*(4), 397-403. http://nopr.niscair.res.in/handle/123456789/7075

Ranjan, P., Ramanathan, A. L., Kumar, A., Singhal, R. K., Datta, D., & Venkatesh, M. (2018). Trace metal distribution, assessment and enrichment in the surface sediments of Sundarban mangrove ecosystem in India and Bangladesh. *Marine pollution bulletin*, *127*, 541-547. https://doi.org/10.1016/j.marpolbul.2017.11.047

Rashedi, S. A., & Siad, A. (2016). Grain size analysis and depositional environment for beach sediments along Abu Dhabi coast, United Arab Emirates. *International Journal Of Scientific & Technology Research*, *5*(07).

Reineck, H. E., & Singh, I. B. (2012). *Depositional sedimentary environments: with reference to terrigenous clastics*. Springer Science & Business Media.

Rubalingeswari, N., Thulasimala, D., Giridharan, L., Gopal, V., Magesh, N. S., & Jayaprakash, M. (2021). Bioaccumulation of heavy metals in water, sediment, and tissues of major fisheries from Adyar estuary, southeast coast of India: An ecotoxicological impact of a metropolitan city. *Marine Pollution Bulletin*, *163*, 111964. https://doi.org/10.1016/j.marpolbul.2020.111964

Saha, M., Sarkar, S. K., & Bhattacharya, B. (2006). Interspecific variation in heavy metal body concentrations in biota of Sunderban mangrove wetland, northeast India. *Environment International*, *32*(2), 203-207. https://doi.org/10.1016/j.envint.2005.08.012

Saha, S. B., Mitra, A., Bhattacharyya, S. B., & Choudhury, A. (2001). Status of sediment with special reference to heavy metal pollution of a brackishwater tidal ecosystem in northern Sundarbans of West Bengal. *Tropical Ecology*, *42*(1), 127-132.

Sahu, B. K. (1964). Depositional mechanisms from the size analysis of clastic sediments. *Journal of Sedimentary Research*, *34*(1), 73-83. https://doi.org/10.1306/74D70FCE-2B21-11D7-8648000102C1865D

Sahu, K. C., & Bhosale, U. (1991). Heavy metal pollution around the island city of Bombay, India. Part I: quantification of heavy metal pollution of aquatic sediments and recognition of environmental discriminants. *Chemical geology*, *90*(3), 263-283. https://doi.org/10.1016/0009-2541(91)90104-Y

Sarkar, S. K., Mondal, P., Biswas, J. K., Kwon, E. E., Ok, Y. S., & Rinklebe, J. (2017). Trace elements in surface sediments of the Hooghly (Ganges) estuary: distribution and contamination risk assessment. *Environmental geochemistry and health*, *39*(6), 1245-1258. https://doi.org/10.1007/s10653-017-9952-3

Schaider, L. A., Senn, D. B., Estes, E. R., Brabander, D. J., & Shine, J. P. (2014). Sources and fates of heavy metals in a mining-impacted stream: temporal variability and the role of iron oxides. *Science of the total environment*, *490*, 456-466. https://doi.org/10.1016/j.scitotenv.2014.04.126

Shah, B. A., Shah, A. V., Mistry, C. B., & Navik, A. J. (2013). Assessment of heavy metals in sediments near Hazira industrial zone at Tapti River estuary, Surat, India. *Environmental Earth Sciences*, *69*(7), 2365-3276. https://doi.org/10.1007/s12665-012-2066-4

Shepard, F. P. (1954). Nomenclature based on sand-silt-clay ratios. *Journal of sedimentary Research*, *24*(3), 151-158. https://doi.org/10.1306/D4269774-2B26-11D7-8648000102C1865D

Siddique, M. A. M., Rahman, M., Rahman, S. M. A., Hassan, M. R., Fardous, Z., Chowdhury, M. A. Z., & Hossain, M. B. (2021). Assessment of heavy metal contamination in the surficial sediments from the lower Meghna River estuary, Noakhali coast, Bangladesh. International Journal of Sediment Research, *36*(3), 384-391. https://doi.org/10.1016/j.ijsrc.2020.10.010

Silva Filho, E. V., Jonathan, M. P., Chatterjee, M., Sarkar, S. K., Sella, S. M., Bhattacharya, A., & Satpathy, K. K. (2011). Ecological consideration of trace element contamination in sediment cores from Sundarban wetland, India. *Environmental Earth Sciences*, *63*(6), 1213-1225. https://doi.org/10.1007/s12665-010-0795-9

Singh, G., Ramanathan, A. L., Santra, S. C., & Ranjan, R. K. (2016). Tidal control on the nutrient variability in Sundarban mangrove ecosystem. *Journal of Applied Geochemistry*, *18*(4), 495-503.

Smith, B. D., Braulik, G., Strindberg, S., Mansur, R., Diyan, M. A. A., & Ahmed, B. (2009). Habitat selection of freshwater-dependent cetaceans and the potential effects of declining freshwater flows and sea-level rise in waterways of the Sundarbans mangrove forest, Bangladesh. *Aquatic Conservation: Marine and Freshwater Ecosystems*, *19*(2), 209-225. https://doi.org/10.1002/aqc.987

Spalding, M. D., Blasco, F., & Field, C. D. (1997). World Atlas of Mangroves. Okinawa, Japan. *International Society for Mangrove Ecosystems (ISME)*, 178.

Stanley, D. J., & Hait, A. K. (2000). Holocene depositional patterns, neotectonics and Sundarban mangroves in the western Ganges-Brahmaputra delta. *Journal of Coastal Research*, 16(1), 26-39.

Strady, E., Dinh, Q. T., Némery, J., Nguyen, T. N., Guédron, S., Nguyen, N. S., Denis, H. & Nguyen, P. D. (2017). Spatial variation and risk assessment of trace metals in water and sediment of the Mekong Delta. *Chemosphere*, *179*, 367-378. https://doi.org/10.1016/j.chemosphere.2017.03.105

Thinh, N. V., Osanai, Y., Adachi, T., Thai, P. K., Nakano, N., Ozaki, A. Kuwahara Y., Kato R., Makio M., & Kurosawa, K. (2018). Chemical speciation and bioavailability concentration of arsenic and heavy metals in sediment and soil cores in estuarine ecosystem, Vietnam. *Microchemical Journal*, *139*, 268-277. https://doi.org/10.1016/j.microc.2018.03.005

Tomlinson, D. L., Wilson, J. G., Harris, C. R., & Jeffrey, D. W. (1980). Problems in the assessment of heavy-metal levels in estuaries and the formation of a pollution index. *Helgoländer meeresuntersuchungen*, *33*(1-4), 566-575.

Turner, A. (2000). Trace metal contamination in sediments from UK estuaries: an empirical evaluation of the role of hydrous iron and manganese oxides. *Estuarine, Coastal and Shelf Science*, *50*(3), 355-371. https://doi.org/10.1006/ecss.1999.0573

Wang, Q., Hong, H., Yang, D., Li, J., Chen, S., Pan, C., Lu, H., Liu, J., & Yan, C. (2020). Health risk assessment of heavy metal and its mitigation by glomalin-related soil protein in sediments along the South China coast. *Environmental Pollution*, *263*, 114565. https://doi.org/10.1016/j.envpol.2020.114565

Woodroffe, C. D., Rogers, K., McKee, K. L., Lovelock, C. E., Mendelssohn, I. A., & Saintilan, N. (2016). Mangrove sedimentation and response to relative sea-level rise. *Annual review of marine science*, *8*, 243-266. https://doi.org/10.1146/annurev-marine-122414-034025

Xie, M., Wang, N., Gaillard, J. F., & Packman, A. I. (2016). Hydrodynamic forcing mobilizes Cu in low-permeability estuarine sediments. *Environmental science & technology*, *50*(9), 4615-4623. https://doi.org/10.1021/acs.est.5b04576

Yang, D., Wang, M., Lu, H., Ding, Z., Liu, J., & Yan, C. (2019). Magnetic properties and correlation with heavy metals in mangrove sediments, the case study on the coast of Fujian, China. *Marine pollution bulletin*, *146*, 865-873. https://doi.org/10.1016/j.marpolbul.2019.07.035

Zaman, S., Bhattacharyya, S. B., Pramanick, P., Raha, A. K., Chakraborty, S., & Mitra, A. (2014). Rising water salinity: A threat to mangroves of Indian Sundarbans. In ed. Abedin A. M., Habiba, U., & Shaw, R. (Eds.), Water *insecurity: a social dilemma, (Community, Environment and Disaster Risk Management, Vol. 13),* (pp 167- 183). Emerald Group Publishing Limited.

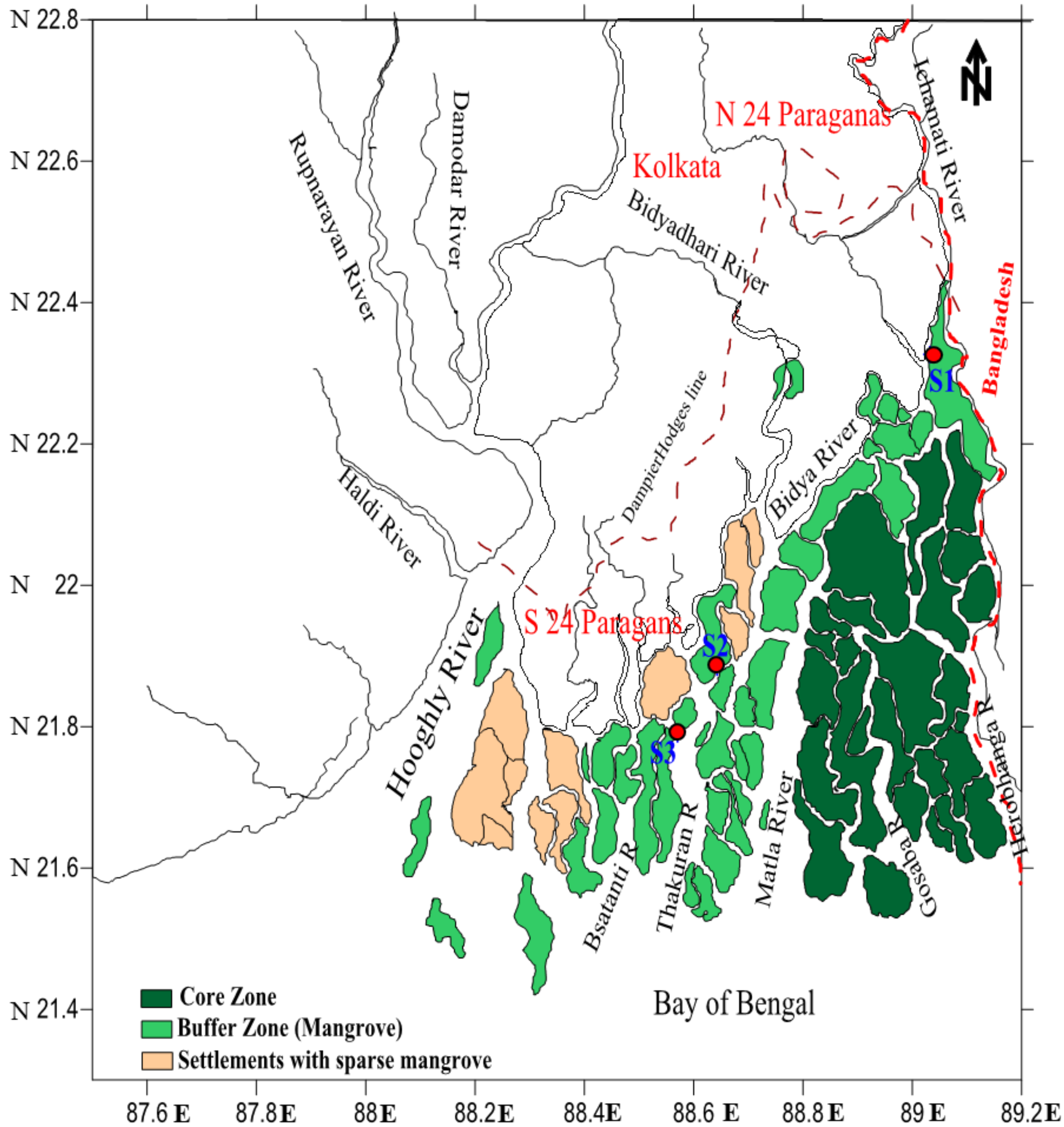

Fig. 1 Map of Sundarban along with three (S1: Sushunia Island, S2: Moipith Island, and S3: Belmati Island) sampling locations.

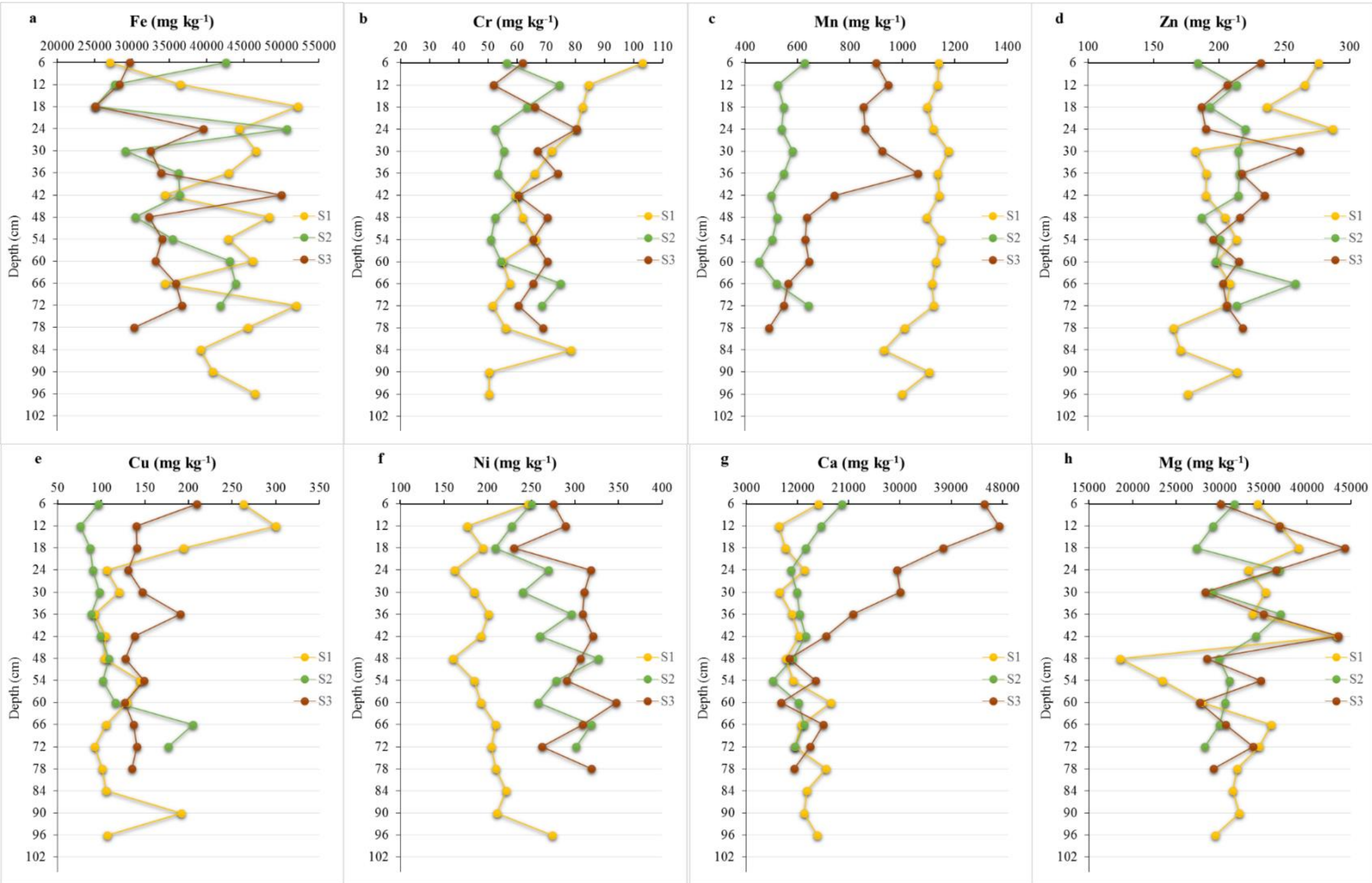

Fig. 2 Vertical distribution of total metal concentrations in the sediment cores collected from the studied locations (S1, S2, and S3).

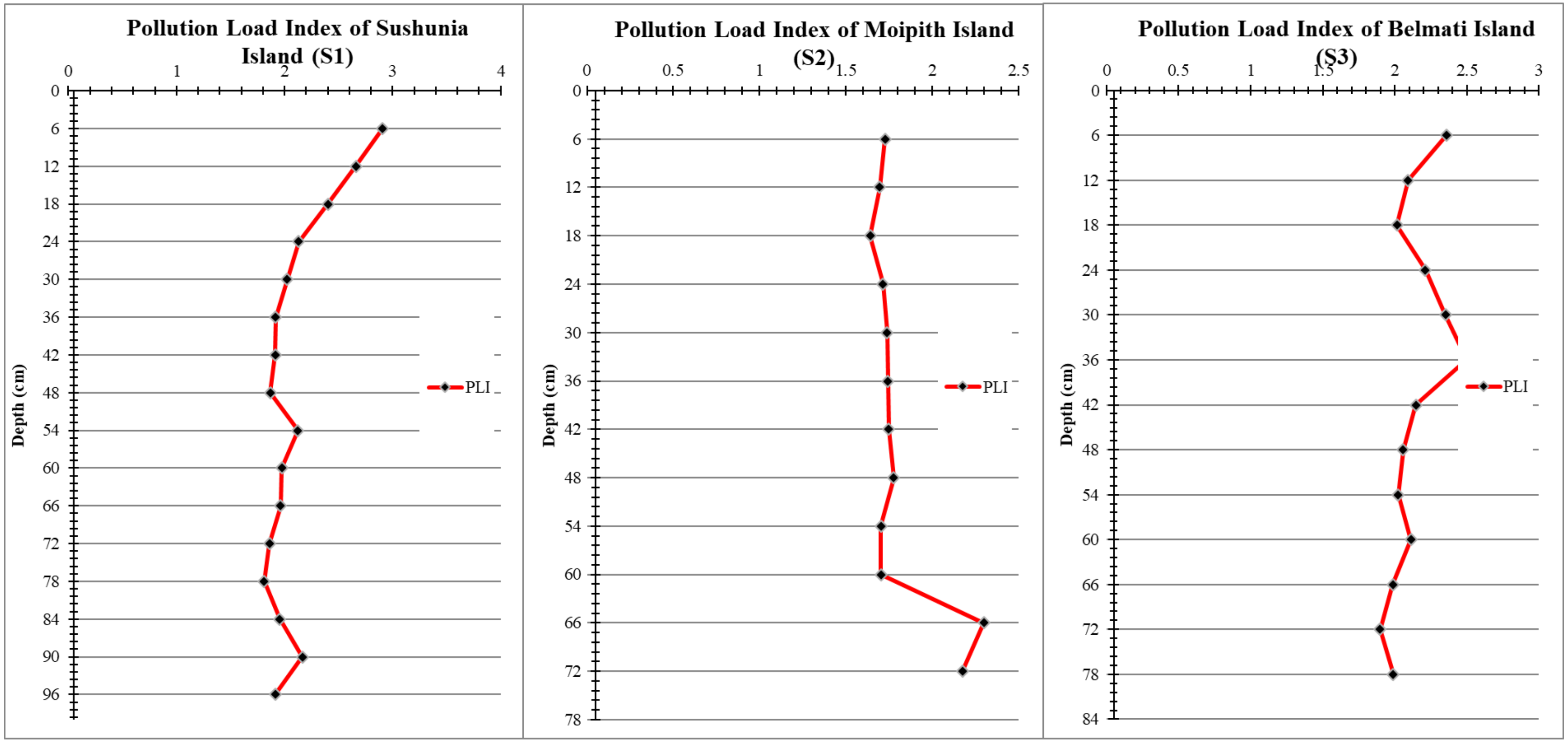

Fig. 3. Pollution Load Index (PLI) in different depths of the sediment cores collected from the studied locations (S1, S2, and S3)

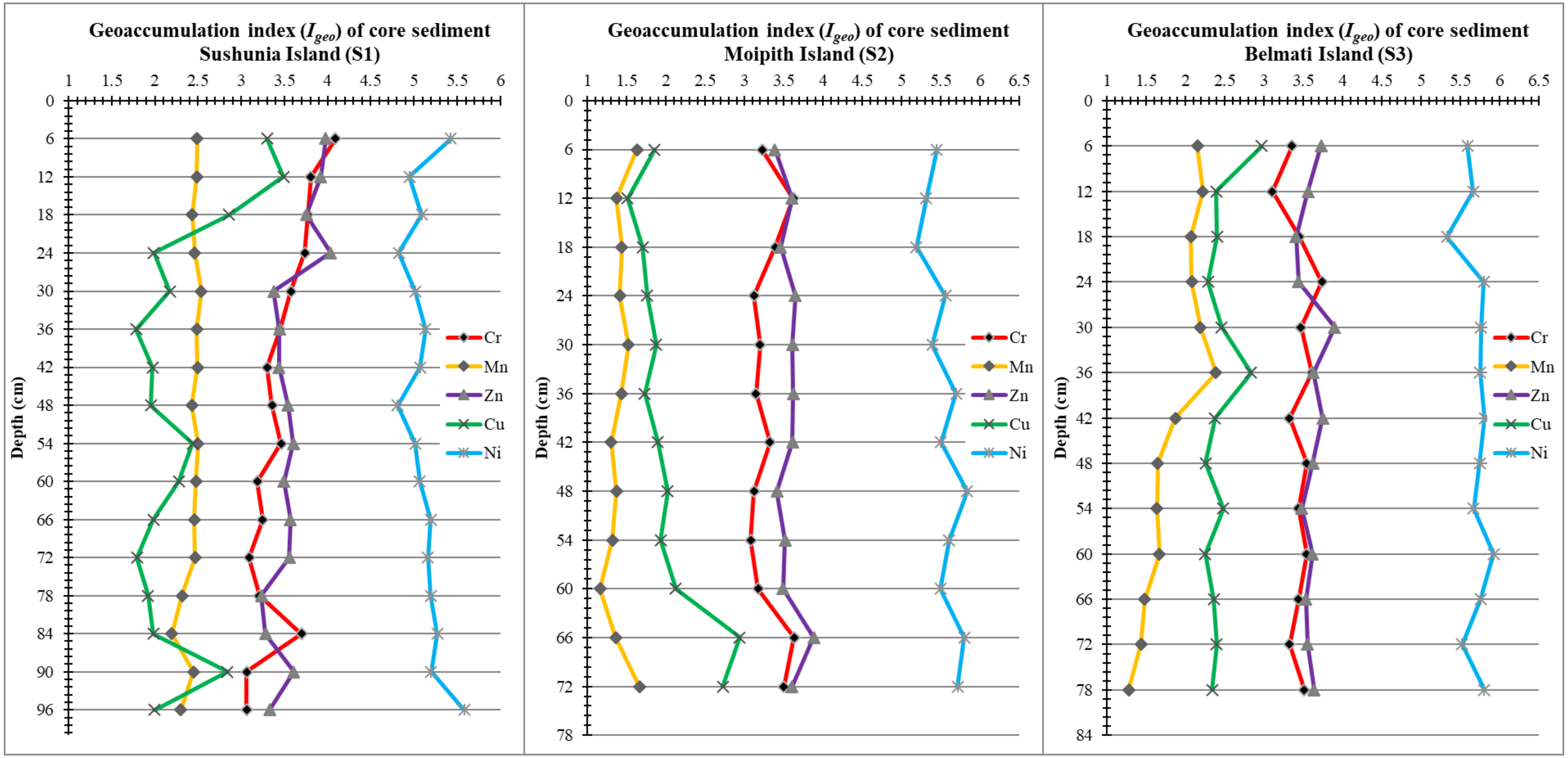

Fig. 4. Geo-accumulation Index (*Igeo*) values of the studied metals at different depths of the sediment cores collected from the studied locations (S1, S2, and S3)

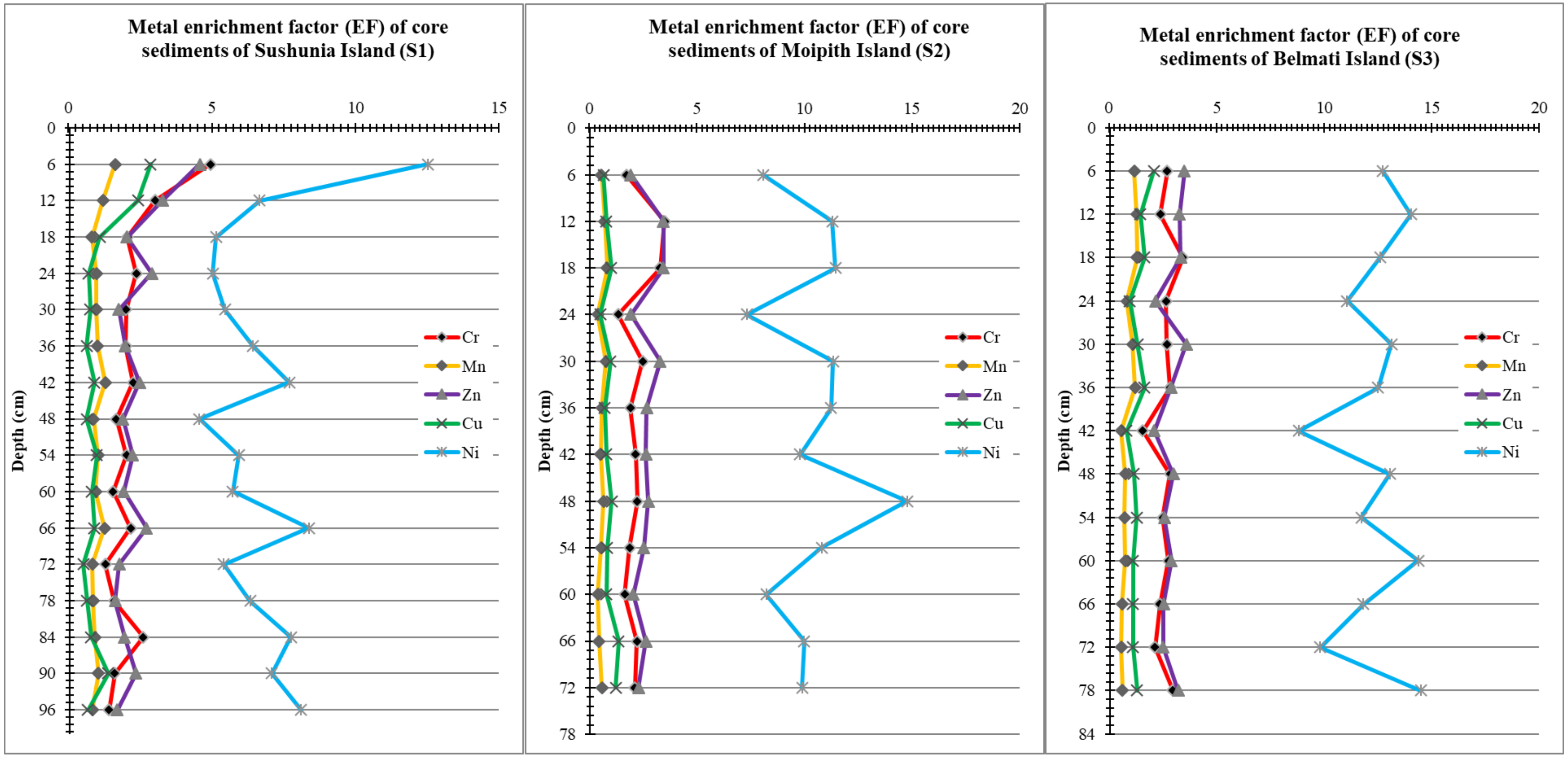

Fig. 5. Enrichment Factor (EF) of the studied metals at different depths of the sediment cores collected from the studied locations (S1, S2, and S3)

Table 1 Linear discriminant function (LDF) analysis of core sediments collected from the studied locations (S1, S2, and S3

Study site	Depth (cm)	Y1	Process	Y2	Process	Y3	Process	Y4	Process
S1	0-6	-5.3	Aeolian process	126.71	Shallow agitated environment	-8.57	Fluvial	5.52	Turbidity current
	6-12	-5.07	Aeolian process	124.17	Shallow agitated environment	-8.59	Fluvial	6.19	Turbidity current
	12-18	-5.02	Aeolian process	119.84	Shallow agitated environment	-5.38	Shallow marine deposit	1.46	Turbidity current
	18-24	-5.05	Aeolian process	123.39	Shallow agitated environment	-6.02	Shallow marine deposit	1.72	Turbidity current
	24-30	-5.32	Aeolian process	130.6	Shallow agitated environment	-9.2	Fluvial	5.59	Turbidity current
	30-36	-4.97	Aeolian process	123.04	Shallow agitated environment	-5.96	Shallow marine deposit	1.85	Turbidity current
	36-42	-5.06	Aeolian process	125.11	Shallow agitated environment	-6.2	Shallow marine deposit	1.82	Turbidity current
	42-48	-5.04	Aeolian process	124.4	Shallow agitated environment	-6.28	Shallow marine deposit	1.92	Turbidity current
	48-54	-5.01	Aeolian process	122.3	Shallow agitated environment	-5.93	Shallow marine deposit	1.83	Turbidity current
	54-60	-5.05	Aeolian process	125.29	Shallow agitated environment	-6.31	Shallow marine deposit	1.73	Turbidity current
	60-66	-4.9	Aeolian process	127.17	Shallow agitated environment	-6.69	Shallow marine deposit	2.21	Turbidity current
	66-72	-5.06	Aeolian process	135.05	Shallow agitated environment	-9.72	Fluvial	5.88	Turbidity current
	72-78	-4.98	Aeolian process	128.26	Shallow agitated environment	-6.74	Shallow marine deposit	1.99	Turbidity current
	78-84	-4.97	Aeolian process	127.26	Shallow agitated environment	-6.73	Shallow marine deposit	2.15	Turbidity current
	84-90	-4.96	Aeolian process	118.45	Shallow agitated environment	-5.35	Shallow marine deposit	1.46	Turbidity current
	90-96	-4.99	Aeolian process	128.38	Shallow agitated environment	-6.75	Shallow marine deposit	1.94	Turbidity current
S2	0-6	-5.27	Aeolian process	143.74	Shallow agitated environment	-13.38	Fluvial	10.07	Fluvial
	6-12	-5.05	Aeolian process	138.68	Shallow agitated environment	-10.66	Fluvial	6.53	Turbidity current
	12-18	-5.42	Aeolian process	140.72	Shallow agitated environment	-13.07	Fluvial	10.14	Fluvial
	18-24	-5.31	Aeolian process	142.83	Shallow agitated environment	-13.28	Fluvial	10.08	Fluvial
	24-30	-5.2	Aeolian process	136.22	Shallow agitated environment	-10.11	Fluvial	5.96	Turbidity current
	30-36	-5.17	Aeolian process	131.28	Shallow agitated environment	-9.37	Fluvial	6.06	Turbidity current
	36-42	-5.06	Aeolian process	137.17	Shallow agitated environment	-10.55	Fluvial	6.73	Turbidity current
	42-48	-5.1	Aeolian process	137.36	Shallow agitated environment	-10.57	Fluvial	6.63	Turbidity current
	48-54	-5.03	Aeolian process	135.93	Shallow agitated environment	-10.33	Fluvial	6.77	Turbidity current
	54-60	-5.64	Aeolian process	133.49	Shallow agitated environment	-12.19	Fluvial	10.25	Fluvial
	60-66	-5.71	Aeolian process	129.79	Shallow agitated environment	-11.8	Fluvial	10.35	Fluvial
	66-72	-6.04	Aeolian process	126.57	Shallow agitated environment	-11.44	Fluvial	9.97	Fluvial
S3	0-6	-5.06	Aeolian process	114.99	Shallow agitated environment	-4.75	Shallow marine deposit	1.08	Turbidity current
	6-12	-5.17	Aeolian process	126.8	Shallow agitated environment	-6.3	Shallow marine deposit	1.52	Turbidity current
	12-18	-5.15	Aeolian process	126.42	Shallow agitated environment	-6.29	Shallow marine deposit	1.45	Turbidity current
	18-24	-4.97	Aeolian process	130.66	Shallow agitated environment	-6.94	Shallow marine deposit	2.23	Turbidity current
	24-30	-5.3	Aeolian process	127.62	Shallow agitated environment	-8.71	Fluvial	5.52	Turbidity current
	30-36	-4.98	Aeolian process	119.31	Shallow agitated environment	-5.49	Fluvial	1.64	Turbidity current

36-42	-5	Aeolian process	123.29	Shallow agitated environment	-6.05	Fluvial	1.92	Turbidity current
42-48	-5.27	Aeolian process	129.22	Shallow agitated environment	-8.96	Fluvial	5.69	Turbidity current
48-54	-5.36	Aeolian process	124.81	Shallow agitated environment	-8.38	Fluvial	5.42	Turbidity current
54-60	-5.24	Aeolian process	128.13	Shallow agitated environment	-8.73	Fluvial	5.59	Turbidity current
60-66	-5.21	Aeolian process	133.26	Shallow agitated environment	-9.43	Fluvial	5.63	Turbidity current
66-72	-5.28	Aeolian process	129.8	Shallow agitated environment	-8.91	Fluvial	5.54	Turbidity current
72-78	-5.01	Aeolian process	123.45	Shallow agitated environment	-5.99	Shallow marine deposit	1.9	Turbidity current

Table 2 Heavy metal concentrations (mg kg^{-1}) in sediments of Sundarban mangrove estuary is compared to estuaries and mangrove systems in different parts of the world.

Ca	**Mg**	**Fe**	**Zn**	**Mn**	**Ni**	**Cr**	**Cu**	**Estuary**
7695-12646.6	18560-44295	25025-52150	165-287	452.5-1176.5	160.5-274	51-103	76-300	Sundarban present study, India
		55000-74000	82.1-150.5	810.0-1220.4	37.4-75.1	120.5-200.5	46.7-84.0	Sundarban (Ram et al., 2018)
		26300-38600	51.39-101.14	200-800	26.34-50.50	55.24-94.86	22.46-75.49	Sundarban, India (Ranjan et. al., 2018)
		24600-35100	55.91-73.44	400-700	26.3-39.23	56.96-78.61	28.65-41.21	Sundarban, Bangladesh (Ranjan et. al., 2018)
52000	197000-219000							Sundarban, India (Rajkumar et. al., 2012)
9000-190000	35000-95000	20.52-139.60	0.28-2.60	20.52-44.60			4.68-9.12	Sundarban, Bangladesh (Islam et. al., 2004)
		19100-25800	197.22-347 .63	200.7-445.85			43.61-79.87	Sundarban, India (Saha et. al., 2001)
		7135-10068	40.9-3448.4					Sundarban, India (Guhathakurta , and Kaviraj, 2000)
		19100-25800	197.22-347 .63	200.7-445.85			43.61-79.87	Sundarban, India (Saha et. al., 2001)
			117.47-178.80		71.13-107.82	48.26-72.40	123.17-170.52	Tapi River estuary, India (Shah et. al., 2013)
			114-273		91-130	29-69		Thane creek, India (Sahu & Bhosale, 1991)
		11144	93.1	1763.3	27.7		11.2	Cauvery estuary, India (Raju et. al., 2012)
			118-136	291-296	93-138.5	95.2-143	93.3-121.1	Niger delta (Ohimain et. al., 2009)
				160-328	12-25		7-43	Tigris river (Rabee et. al., 2011)
		662.05-1463		982.57-2527.10	9.75-21.28	6.61-14.92		Ondo coast, Nigeria (Adeboale et. al., 2009)
			5.97-188.89		4.55-26.21	30.75-99.62	4.18-23.24	Fujian, China (Yanga et al., 2019)
			59.5.-70.90			53.60-84.20	14.30-26.30	Fujian, China (Liu et al., 2014)

14100-22600	61.50-100.80	600-1300		24.70-38.60	30.10-67.80	Ba-Lat estuary, Vietnam (Thinh et al., 2018)
38500-61100	59-174	235-1469	41-90	74-184	15-41	Can Gio District, Ho Chi Min City, Vietnam (Dung et al., 2019)
57300-73800	185-446	646-2485	27-179	391.8-1272.3	167-522	Adyar estuary, southeast coast of India (Rubalingeswari et al., 2021)
	20.64-106.87	52.87-730.23	6.37-24.11	19.17-56.80	10.03-24.89	South China coast (Wang et al., 2020)
210-2420	4.90-97.75			0.045-18.60	0.01-16.60	Meghna River estuary, Noakhali coast, Bangladesh (Siddque et al., 2021)

Supplementary Information

Sedimentation of metals in Sundarban mangrove ecosystem: Dominant drivers and environmental risks

Jayjit Majumdar[1]*, Jayanta Kumar Biswas[1,2]*, Subhas Chandra Santra[3], AL. Ramanathan[4] and Filip M. G. Tack[5]

[1]Department of Ecological Studies, University of Kalyani, Kalyani, Nadia, West Bengal - 741235, India

[2]International Centre for Ecological Engineering, University of Kalyani, Kalyani, Nadia, West Bengal - 741235, India

[3]Department of Environmental Science, University of Kalyani, Kalyani, Nadia, West Bengal - 741235, India

[4]School of Environmental Sciences, Jawaharlal Nehru University, New Delhi- 110067, India

[5]Department of Green Chemistry and Technology, Ghent University, Ghent, Belgium

*Corresponding authors (J. Majumdar, e-mail: jayjitmajumdar@gmail.com; J.K. Biswas, e-mail: biswajoy2008@gmail.com)

Supplementary Table 1 Grain fractions of the core sediment samples in the different depths

Study	Depth	Initial	Grain size fractions (g)	Recovery

site (Sediment cores)	[cm]	Weight (g)	>250 µm	>125 µm	>63 µm	>37 µm	<37 µm	percentage
S1	0-6	50	17.85	7.63	13.33	9.51	0.99	98.62
	6-12	50	20.77	11.35	12.15	2.68	2.76	99.42
	12-18	50	15.45	4.38	18.58	10.38	0.78	99.14
	18-24	50	17.31	5.19	12.83	13.23	0.84	98.80
	24-30	50	19.98	5.60	8.80	14.16	0.68	98.44
	30-36	50	17.42	5.89	13.66	11.43	1.25	99.30
	36-42	50	15.06	5.94	13.18	13.40	1.65	98.46
	42-48	50	18.44	5.92	10.43	13.44	1.05	98.56
	48-54	50	18.13	6.25	12.23	11.93	0.67	98.42
	54-60	50	18.17	3.86	10.73	14.99	1.19	97.88
	60-66	50	20.03	4.73	10.25	12.00	2.54	99.10
	66-72	50	19.91	5.38	9.12	11.44	3.43	98.56
	72-78	50	17.96	4.50	9.13	14.99	2.64	98.44
	78-84	50	19.60	5.23	8.90	13.78	2.25	99.52
	84-90	50	19.62	4.23	15.83	9.04	0.89	99.22
	90-94	50	18.23	4.24	8.55	15.84	2.62	98.96
S2	0-6	100	50.03	11.20	2.67	28.18	7.65	99.73
	6-12	100	46.04	12.57	3.81	27.79	8.83	99.04
	12-18	100	53.47	11.04	4.10	26.72	4.30	99.63
	18-24	100	49.73	12.40	2.41	27.56	6.44	98.54
	24-30	100	41.23	12.30	3.91	35.34	5.66	98.44
	30-36	100	41.82	12.77	19.50	21.34	3.64	99.07
	36-42	100	48.22	13.11	6.63	23.89	7.25	99.10
	42-48	100	47.54	13.80	3.60	27.24	6.98	99.16
	48-54	100	48.08	14.07	10.10	20.51	6.82	99.58
	54-60	100	52.20	12.27	15.74	17.10	1.66	98.97
	60-66	100	55.72	16.05	12.58	12.39	1.64	98.38
	66-70	100	51.42	10.94	27.38	8.67	1.01	99.42
S3	0-6	50	15.25	6.05	19.35	8.33	0.56	99.08
	6-12	50	13.38	5.56	8.86	19.09	1.65	97.08
	12-18	50	15.25	5.22	7.20	20.22	1.12	98.02
	18-24	50	13.19	6.30	12.04	12.12	4.38	96.06
	24-30	50	19.12	6.47	12.42	11.00	0.61	99.24
	30-36	50	17.66	6.81	14.71	9.09	1.04	98.62
	36-42	50	17.04	7.06	12.26	11.75	1.15	98.52
	42-48	50	18.99	6.80	10.97	11.43	0.91	98.20
	48-54	50	18.72	7.23	13.68	9.33	0.48	98.88
	54-60	50	18.26	6.98	13.06	9.60	1.40	98.60
	60-66	50	17.62	6.79	8.79	13.15	2.38	97.46
	66-72	50	16.72	7.69	11.47	11.72	1.21	97.62
	72-78	50	15.24	7.27	13.78	11.39	1.42	98.20

Supplementary Table 2 Statistical analysis of grain size parameters of core sediments collected from the studied locations (S1, S2, and S3)

Study Site	Depth [cm]	Mean (ϕ)	Std. Dev. (σ1)	Skewness (Sk_1)	Kurtosis (K_G)	Mean	Sorting	Skewness	Kurtosis	Sediment type
S1	0-6	3.008	1.02	0.105	0.577	Very Fine Sand	Poorly Sorted	Fine Skewed	Very Platykurtic	Very Coarse Silty Medium Sand
	6-12	2.869	0.981	0.173	0.633	Fine Sand	Moderately Sorted	Fine Skewed	Very Platykurtic	Very Coarse Silty Medium Sand
	12-18	3.301	1.021	-0.53	0.577	Very Fine Sand	Poorly Sorted	Very Coarse Skewed	Very Platykurtic	Very Coarse Silty Very Fine Sand
	18-24	3.328	1.06	-0.467	0.547	Very Fine Sand	Poorly Sorted	Very Coarse Skewed	Very Platykurtic	Very Coarse Silty Medium Sand
	24-30	3.054	1.069	0.149	0.532	Very Fine Sand	Poorly Sorted	Fine Skewed	Very Platykurtic	Very Coarse Silty Medium Sand
	30-36	3.309	1.052	-0.465	0.571	Very Fine Sand	Poorly Sorted	Very Coarse Skewed	Very Platykurtic	Very Coarse Silty Medium Sand
	36-42	3.36	1.075	-0.456	0.547	Very Fine Sand	Poorly Sorted	Very Coarse Skewed	Very Platykurtic	Very Coarse Silty Medium Sand
	42-48	3.32	1.069	-0.432	0.541	Very Fine Sand	Poorly Sorted	Very Coarse Skewed	Very Platykurtic	Very Coarse Silty Medium Sand
	48-54	3.295	1.045	-0.461	0.562	Very Fine Sand	Poorly Sorted	Very Coarse Skewed	Very Platykurtic	Very Coarse Silty Medium Sand
	54-60	3.354	1.084	-0.45	0.526	Very Fine Sand	Poorly Sorted	Very Coarse Skewed	Very Platykurtic	Very Coarse Silty Medium Sand
	60-66	3.33	1.096	-0.395	0.551	Very Fine Sand	Poorly Sorted	Very Coarse Skewed	Very Platykurtic	Very Coarse Silty Medium Sand
	67-72	3.089	1.116	0.176	0.552	Very Fine Sand	Poorly Sorted	Fine Skewed	Very Platykurtic	Very Coarse Silty Medium Sand
	72-78	3.379	1.113	-0.412	0.524	Very Fine Sand	Poorly Sorted	Very Coarse Skewed	Very Platykurtic	Very Coarse Silty Medium Sand
	78-84	3.34	1.099	-0.392	0.533	Very Fine Sand	Poorly Sorted	Very Coarse Skewed	Very Platykurtic	Very Coarse Silty Medium Sand
	84-90	3.251	1.011	-0.52	0.571	Very Fine Sand	Poorly Sorted	Very Coarse Skewed	Very Platykurtic	Very Coarse Silty Medium Sand
	90-94	3.385	1.116	-0.415	0.518	Very Fine Sand	Poorly Sorted	Very Coarse Skewed	Very Platykurtic	Very Coarse Silty Medium Sand

Supplementary Table 2 continued

Study Site	Depth [cm]	Mean (ϕ)	Std. Dev. (σ1)	Skewness (Sk_1)	Kurtosis (K_G)	Mean	Sorting	Skewness	Kurtosis	Sediment type
S2	0-6	2.783	1.142	0.857	0.52	Fine Sand	Poorly Sorted	Very Fine Skewed	Very Platykurtic	Very Coarse Silty Medium Sand
	6-12	3.067	1.151	0.302	0.518	Very Fine Sand	Poorly Sorted	Very Fine Skewed	Very Platykurtic	Very Coarse Silty Medium Sand
	12-18	2.74	1.102	0.862	0.529	Fine Sand	Poorly Sorted	Very Fine Skewed	Very Platykurtic	Very Coarse Silty Medium Sand
	18-24	2.771	1.13	0.857	0.523	Fine Sand	Poorly Sorted	Very Fine Skewed	Very Platykurtic	Very Coarse Silty Medium Sand
	24-30	3.094	1.132	0.226	0.504	Very Fine Sand	Poorly Sorted	Fine Skewed	Very Platykurtic	Very Coarse Silty Medium Sand
	30-36	3.017	1.066	0.189	0.573	Very Fine Sand	Poorly Sorted	Fine Skewed	Very Platykurtic	Very Coarse Silty Medium Sand
	36-42	3.022	1.127	0.319	0.54	Very Fine Sand	Poorly Sorted	Very Fine Skewed	Very Platykurtic	Very Coarse Silty Medium Sand
	42-48	3.035	1.133	0.314	0.526	Very Fine Sand	Poorly Sorted	Very Fine Skewed	Very Platykurtic	Very Coarse Silty Medium Sand
	48-54	3.003	1.11	0.306	0.566	Very Fine Sand	Poorly Sorted	Very Fine Skewed	Very Platykurtic	Very Coarse Silty Medium Sand
	54-60	2.641	1.007	0.848	0.574	Fine Sand	Poorly Sorted	Very Fine Skewed	Very Platykurtic	Very Coarse Silty Medium Sand
	60-66	2.578	0.959	0.851	0.595	Fine Sand	Moderately Sorted	Very Fine Skewed	Very Platykurtic	Very Coarse Silty Medium Sand
	67-72	2.58	0.929	0.832	0.546	Fine Sand	Moderately Sorted	Very Fine Skewed	Very Platykurtic	Moderately Sorted Medium Sand

Supplementary Table 2 continued

Study	Depth	Mean	Std. Dev.	Skewness	Kurtosis	Mean	Sorting	Skewness	Kurtosis	Sediment type

Site	[cm]	(ϕ)	(σ1)	(Sk_1)	(K_G)					
S3	0-6	3.244	0.975	-0.581	0.576	Very Fine Sand	Moderately Sorted	Very Coarse Skewed	Very Platykurtic	Very Coarse Silty Very Fine Sand
	6-12	3.429	1.101	-0.478	0.511	Very Fine Sand	Poorly Sorted	Very Coarse Skewed	Very Platykurtic	Very Coarse Silty Medium Sand
	12-18	3.417	1.101	-0.48	0.503	Very Fine Sand	Poorly Sorted	Very Coarse Skewed	Very Platykurtic	Very Coarse Silty Medium Sand
	18-24	3.423	1.129	-0.398	0.547	Very Fine Sand	Poorly Sorted	Very Coarse Skewed	Very Platykurtic	Very Coarse Silty Medium Sand
	24-30	3.02	1.032	0.113	0.567	Very Fine Sand	Poorly Sorted	Fine Skewed	Very Platykurtic	Very Coarse Silty Medium Sand
	30-36	3.257	1.014	-0.499	0.578	Very Fine Sand	Poorly Sorted	Very Coarse Skewed	Very Platykurtic	Very Coarse Silty Medium Sand
	36-42	3.308	1.053	-0.45	0.565	Very Fine Sand	Poorly Sorted	Very Coarse Skewed	Very Platykurtic	Very Coarse Silty Medium Sand
	42-48	3.029	1.048	0.137	0.566	Very Fine Sand	Poorly Sorted	Fine Skewed	Very Platykurtic	Very Coarse Silty Medium Sand
	48-54	2.983	1.002	0.098	0.569	Fine Sand	Poorly Sorted	Symmetrical	Very Platykurtic	Very Coarse Silty Medium Sand
	54-60	3.022	1.036	0.112	0.58	Very Fine Sand	Poorly Sorted	Fine Skewed	Very Platykurtic	Very Coarse Silty Medium Sand
	60-66	3.097	1.098	0.146	0.539	Very Fine Sand	Poorly Sorted	Fine Skewed	Very Platykurtic	Very Coarse Silty Medium Sand
	67-72	3.061	1.055	0.115	0.564	Very Fine Sand	Poorly Sorted	Fine Skewed	Very Platykurtic	Very Coarse Silty Medium Sand
	72-78	3.323	1.053	-0.462	0.574	Very Fine Sand	Poorly Sorted	Very Coarse Skewed	Very Platykurtic	Very Coarse Silty Medium Sand

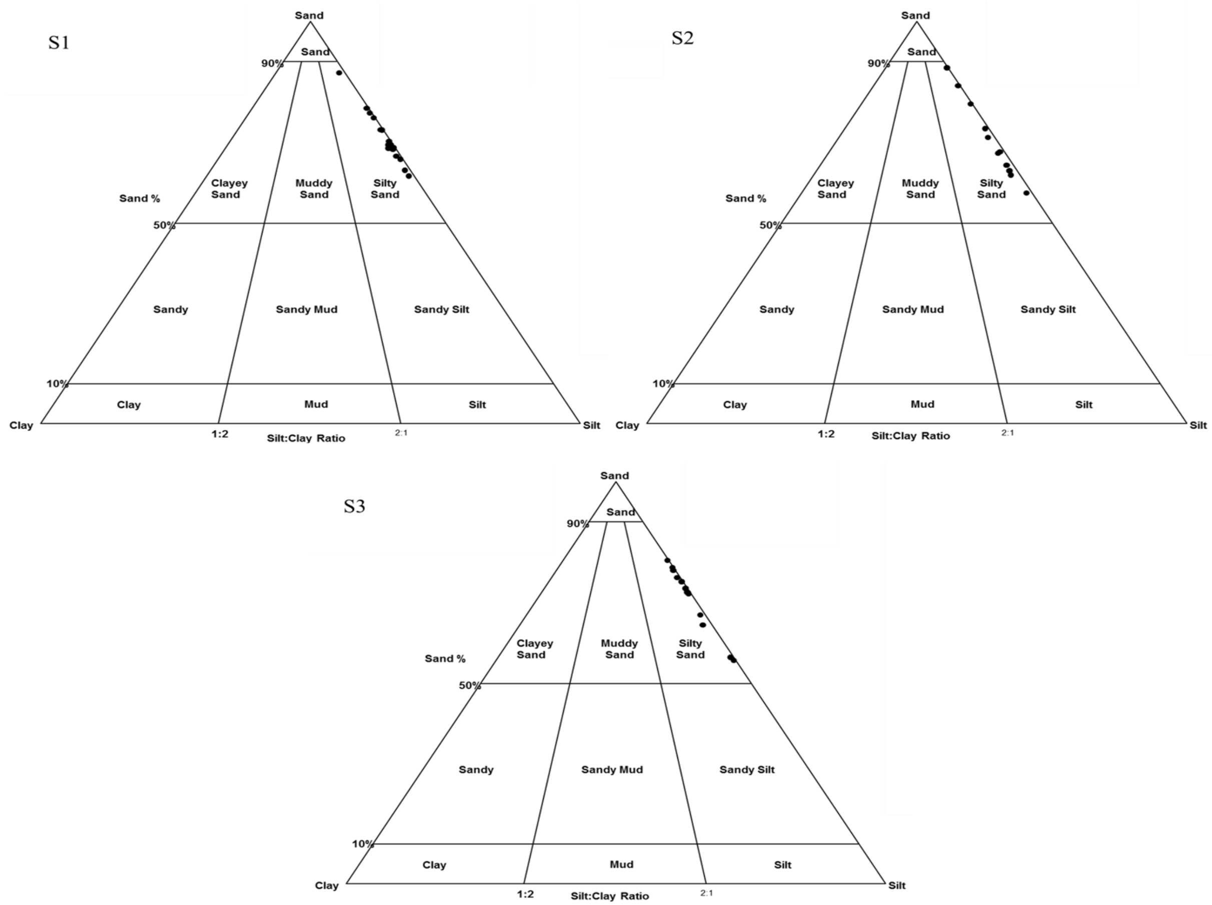

Supplementary Fig. 1 Ternary diagram showing the textural configuration at different depths of the core sediments collected from the studied locations (S1, S2, and S3).